



Hybrid simultaneous whole-body 2-[¹⁸F]FDG-PET/MRI imaging in newly diagnosed multiple myeloma: first diagnostic performance and clinical added value results

Bastien Jamet¹ · Thomas Carlier^{1,2} · Clément Bailly^{1,2} · Caroline Bodet-Milin^{1,2} · Aurélien Monnet⁴ · Eric Frampas⁵ · Cyrille Touzeau^{2,3} · Philippe Moreau^{2,3} · Françoise Kraeber-Bodere^{1,2}

Received: 7 September 2022 / Revised: 10 January 2023 / Accepted: 22 February 2023 / Published online: 6 April 2023

© The Author(s), under exclusive licence to European Society of Radiology 2023

Abstract

Objectives Mixing diagnostic and prognostic data provided by whole-body MRI (WB-MRI) and 2-¹⁸F-fluorodeoxyglucose (2-[¹⁸F]FDG) positron emission tomography (2-[¹⁸F]FDG-PET) from a single simultaneous imaging technique for newly diagnosed multiple myeloma (NDMM) initial workup seems attractive. However, to date, the published data are scarce and this possibility has not been fully explored. In this prospective study, we aimed to explore the diagnostic performance and added clinical value of WB-2-[¹⁸F]FDG-PET/MRI imaging in NDMM.

Methods All patients with confirmed NDMM at the Nantes University Hospital were prospectively enrolled in this study and underwent WB-2-[¹⁸F]FDG-PET/MRI imaging on a 3-T Biograph mMR before receiving treatment. Before imaging, they were considered either as symptomatic or as smoldering MM (SMM). Diagnostic performance of global WB-2-[¹⁸F]FDG-PET/MRI imaging, as well as PET and MRI separately for FL and diffuse BMI detection, was assessed and compared in each group. PET-based (maximal standardized uptake value, SUV_{max}) and MRI-based (mean apparent diffusion coefficient value, ADC_{mean}) quantitative features were collected for FL/para-medullary disease (PMD)/bone marrow and were compared.

Results A total of 52 patients were included in this study. PET and MRI were equally effective at detecting patients with FL (69% vs. 75%) and with diffuse BMI (62% for both) in the symptomatic MM group. WB-2-[¹⁸F]FDG-PET/MRI imaging detected FL in 22% of patients with SMM (with a higher diagnostic performance for MRI), resulting in a significant impact on clinical management in this population. SUV_{max} and ADC_{mean} quantitative features were weakly or not correlated.

Conclusions WB-2-[¹⁸F]FDG-PET/MRI could represent the next-generation imaging modality for MM.

Key Points

- Whole-body 2-[¹⁸F]FDG-PET/MRI imaging detected at least one focal bone lesion in 75% of patients with symptomatic multiple myeloma, and PET and MRI were equally effective at identifying patients with a focal bone lesion.
- Whole-body 2-[¹⁸F]FDG-PET/MRI imaging detected a focal bone lesion in 22% of patients with smoldering multiple myeloma (with a higher diagnostic performance for MRI).
- MRI had a significant impact on clinical management of smoldering multiple myeloma.

Keywords Multiple myeloma · Positron emission tomography · Magnetic resonance imaging · Clinical decision-making · Diagnostic techniques, radioisotope

✉ Bastien Jamet
bastien.jamet@chu-nantes.fr

¹ Nuclear Medicine Department, University Hospital, 1 Place Ricordeau, 44093 Nantes, France

² Nantes Université, Univ Angers, INSERM, CNRS, CRCI2NA, F-44000 Nantes, France

³ Haematology Department, University Hospital, Nantes, France

⁴ Siemens, France

⁵ Radiology Department, University Hospital, Nantes, France

Abbreviations

2- ¹⁸ F]FDG	2- ¹⁸ F-fluorodeoxyglucose
ADC	Apparent diffusion coefficient
BMI	Bone marrow involvement
CT	Computed tomography
DCE	Dynamic contrast enhanced
DWI	Diffusion-weighted imaging
EMD	Extra-medullary disease
FL	Focal bone lesion
IMWG	International Myeloma Working Group
MDE	Myeloma defining event
MM	Multiple myeloma
MRAC	Magnetic resonance attenuation correction
NDMM	Newly diagnosed multiple myeloma
PET	Positron emission tomography
PMD	Para-medullary disease
ROC	Receiver-operating characteristic
ROI	Region of interest
SMM	Smoldering multiple myeloma
SUV _{max}	Maximal standardized uptake value
WB-2- ¹⁸ F]FDG-PET/MRI	Whole-body 2- ¹⁸ F-fluorodeoxyglucose-positron emission tomography coupled with magnetic resonance imaging

Introduction

Modern imaging techniques are now widely used in newly diagnosed multiple myeloma (NDMM) in order to detect bone disease which is a primary criterion to initiate therapy [1]. In the latest International Myeloma Working Group (IMWG) imaging guidelines [2], both whole-body MRI (WB-MRI) and 2-¹⁸F-fluorodeoxyglucose (2-¹⁸F]FDG) positron emission tomography (PET) with computed tomography (CT) imaging techniques can be performed at initial workup.

WB-MRI is highly sensitive for identifying focal bone lesion (FL) — a myeloma-defining event (MDE) — especially at the early smoldering multiple myeloma (SMM) phase [3, 4]. Moreover, MRI imaging does not expose patients to radiation and allows differential diagnosis between osteoporotic and pathological fractures as well as spinal cord compression complication detection. On

the other hand, 2-¹⁸F]FDG-PET imaging is also a sensitive imaging technique for FL detection at baseline [5, 6] and provides added crucial prognostic data from the outset [6–10]. Thus, mixing these diagnostic and prognostic data in a single imaging technique seems attractive.

New hybrid simultaneous PET/MRI imaging has emerged over recent years and these devices can substitute the usual CT scan with an MRI scan coupled with PET imaging. The theoretical and practical potential of performing single simultaneous WB-2-¹⁸F]FDG-PET/MRI imaging for NDMM is high, but to date, this has not been fully explored and published data are scarce.

In this prospective study, we aimed to describe our imaging protocol as well as to explore the diagnostic performance and added clinical value of WB-2-¹⁸F]FDG-PET/MRI imaging in NDMM.

Materials and methods

Patients

All patients with confirmed NDMM according to IMWG criteria [1] at the Nantes University Hospital were prospectively enrolled in this study and underwent WB-2-¹⁸F]FDG-PET/MRI imaging between May and December 2021 before receiving treatment. These patients were included in the MYRACLE protocol study as well [11].

Patients with NDMM were considered as symptomatic before the WB-2-¹⁸F]FDG-PET/MRI imaging if any one or more MDE were present: end organ damage attributed to the MM; hypercalcemia, renal insufficiency, anemia, osteolytic bone lesions, and/or biomarkers of malignancy: clonal bone marrow plasma cell percentage $\geq 60\%$, involved/uninvolved serum free light chain ratio ≥ 100 .

If no MDE was present at baseline before the WB-2-¹⁸F]FDG-PET/MRI imaging, patients were regarded as SMM.

This prospective study was approved by a local institutional review board committee. Informed consent was obtained from all individual participants included in the study.

PET/MRI device and imaging protocol

Imaging was carried out using a 3-T Biograph mMR (Siemens).

Simultaneous WB-PET and WB-MRI imaging (from the top of the head down to under the knees or through to the feet, with arms along the body) was performed 55 to 75 min after the 2-¹⁸F]FDG injection (3 MBq/kg). PET data were reconstructed using the 3D ordinary Poisson ordered-subset expectation maximization provided by the manufacturer with 3 iterations, 21 subsets, and Gaussian post-smoothing of

4-mm full width at half maximum (voxel size: $2.1 \times 2.1 \times 2.0$ mm³). The MRI imaging protocol included, as recommended by the international guidelines [12]:

- WB 3D Gradient Echo T1-weighted magnetic resonance attenuation correction (MRAC) for PET reconstruction and generating fat fraction maps.
- Whole-spine sagittal T1 TSE-DIXON (slice thickness 4 mm, FOV 280 mm, matrix 256, TR/TE: 750/10 ms) and T2 TSE-STIR weighted (slice thickness 3.5 mm, FOV 280 mm, matrix 320, TR/TE: 4000/59 ms).
- WB axial diffusion-weighted (DWI) with 2 *b* values (50 and 800 s/mm²) and apparent diffusion coefficient (ADC) calculation and 3D-MIP reconstructions of highest *b*-value images, WB axial T2 TSE-STIR weighted (5-mm contiguous slices, FOV 450 mm, matrix 256, TR/TE: 4300/70 ms).

Moreover, dynamic contrast enhanced (DCE)–MRI was performed as previously proposed [13] by injecting a bolus of gadolinium contrast agent of 0.2 mL/kg at an injection rate of 3–5 mL/s. This protocol consists of a 3D acquisition repeated every 3.1 s by use of 3D Gradient Echo sequence (slice thickness 2 mm, FOV 300 mm, matrix 192, TR/TE: 2.32/0.72 ms, flip angle = 12°, 40 repetitions) of the lumbar spine and the sacrum.

PET/MRI assessment

All patients fasted for at least 6 h before the PET/MRI imaging. No dexamethasone was administered within 12 h before the imaging. Blood glucose levels were measured before 2-[¹⁸F]FDG injection with a preferred glycemia level ≤ 150 mg/dL; up to 200 mg/dL was allowed. No insulin was administered within 2 h before 2-[¹⁸F]FDG injection. Patients could receive a mild sedative orally before 2-[¹⁸F]FDG injection as needed. Absolute contraindications to MRI imaging were systematically queried before imaging.

PET images were interpreted by a team of nuclear medicine physicians with extensive experience in MM. FL was defined as foci within bones more intense than normal bone marrow background and present on at least two consecutive slices. Diffuse bone marrow involvement (BMI) was defined as an uptake (homogeneous or heterogeneous) in the axial and appendicular skeleton higher than liver uptake. Extra-medullary disease (EMD) was considered as soft tissue invasion without contiguous bone involvement and paramedullary disease (PMD) as soft tissue invasion with contiguous bone involvement. The number of FL/PMD/EMD lesions was quantified for each as follows: (*N* = 1), (*N* = 2), (*N* = 3), (*N* = 4), (*N* = 5 to 10), and (*N* > 10), as guided by the IMPeTUs criteria

[14]. Localizations of the most intense 2-[¹⁸F]FDG uptake were identified and the whole-body maximal standardized uptake value (SUV_{max}) was calculated for FL (SUV_{max}FL), PMD (SUV_{max}PMD), and EMD (SUV_{max}EMD) lesions, using the body weight corrected formulation, for each PET dataset. SUV_{max}BM (SUV_{max} of bone marrow) was measured with regions of interest (ROIs) of similar size (4 cm³) placed inside the vertebral body of L4 or L5 on a single slice (preferentially sagittal) excluding FL when present at this level.

MRI assessment was performed as recommended by international guidelines [12]. FLs greater than 5 mm with appropriate signal characteristics were considered as focal active disease. As for PET imaging, EMD was considered as soft tissue invasion without contiguous bone involvement and PMD as soft tissue invasion with contiguous bone involvement. The number of FL/PMD/EMD lesions was quantified for each as follows: (*N* = 1), (*N* = 2), (*N* = 3), (*N* = 4), (*N* = 5 to 10), and (*N* > 10). True positivity of detected FL was confirmed with follow-up scans.

Diffuse BMI was considered when a diffuse decreased signal on T1-in phase-DIXON weighted and diffuse increased signal throughout the marrow (relative to normal adjacent muscle) on high *b*-value images were present [15].

Mean values of apparent diffusion coefficient (ADC_{mean}) were recorded for FL (ADC_{mean}FL), PMD (ADC_{mean}PMD), and EMD (ADC_{mean}EMD) lesions with ROIs greater than 1cm² of similar size placed inside the most intense 2-[¹⁸F]FDG uptake lesions for each patient. Moreover, ADC_{mean}BM (ADC_{mean} of bone marrow) was registered as for PET imaging with ROIs of 4cm² placed within the vertebral body of L4 or L5 on a single axial slice excluding FL when present at this level.

All MRI images were interpreted by radiologists with extensive experience and specialized skills in osteo-articular imaging. Next, a group of nuclear medicine physicians and radiologists reviewed the imaging outcomes to establish a consensus.

Statistical analysis

Fisher's exact test was used to assess the differences in detecting FLs and diffuse BMI between PET and MRI. The correlation between continuous quantitative variables extracted from PET and MRI was derived using the Spearman rank correlation coefficient. The optimal MRI-based ADC_{mean}BM cut-off value to detect BMI on MRI was performed by receiver-operating characteristic (ROC) analysis using the Youden index and considering PET results as the gold standard. Statistical analyses were performed using R version 4.0.3.

Table 1 Patient's clinical and biological characteristics

Variable	Symptomatic MM <i>n</i> = 16	SMM <i>n</i> = 36
Median age	66 (39 to 85)	66 (32 to 86)
Male	11/16 (69%)	15/36 (42%)
R-ISS I	5/16	N/A
R-ISS II	6/16	N/A
R-ISS III	5/16	N/A
Type of monoclonal Ig or free lights chains		
IgGκ	6/16 (37.5%)	13/36 (36%)
IgGλ	2/16 (12.5%)	12/36 (33%)
K	3/16 (19%)	1/36 (3%)
IgAλ	2/16 (12.5%)	1/36 (3%)
Λ	1/16 (6%)	1/36 (3%)
IgAκ	2/16 (12.5%)	8/36 (22%)
Median serum monoclonal Ig (g/l)	20 (15 to 64)	20 (3 to 35)
Median bone marrow plasma cells (%)	12 (10 to 89)	14 (9 to 81)

MM, multiple myeloma; R-ISS, revised international staging system; N/A, not applicable

Results

Patients

Fifty-two patients with NDMM were consecutively included. Thirty-six (69%) of them had SMM and 16 (31%) symptomatic disease as defined above. Table 1 reports the patient's clinical and biological characteristics.

Among symptomatic MM patients before the WB-2-¹⁸F]FDG-PET/MRI imaging, 6% had hypercalcemia, 31% renal insufficiency, 69% anemia, and 38% bone disease. Three patients had only a biomarker of malignancy (involved/uninvolved serum free light chain ratio ≥ 100) without end organ damage attributed to the MM.

PET/MRI assessment

Total acquisition time was approximately 1 h for each patient. Acquisition was stopped for one patient due to pain; only a subset of images was obtained for this patient.

The performance of WB-2-¹⁸F]FDG-PET/MRI imaging for FL and diffuse BMI detection is reported in Table 2. In the whole population, WB-2-¹⁸F]FDG-PET/MRI imaging detected diffuse BMI and at least one FL in 26/52 (50%) and 20/52 (38%) of patients respectively.

In symptomatic MM patients, FL and diffuse BMI detection rates were roughly equal between PET and MRI. WB-2-¹⁸F]FDG-PET/MRI imaging detected FL in 75% of patients and diffuse BMI in 62% of patients. Among patients with FL (69% for PET and 75% for MRI, $p = 0.5$), MRI identified more FLs (3 patients more with > 10FL and one more with 5 to 10 FL, Table 3).

In the SMM population, WB-2-¹⁸F]FDG-PET/MRI imaging identified FL in 8/36 (22%) of patients (Figs. 1 and 2), leading to an impact on clinical management. Four/36 (11%) of these patients had FL only detected by MRI (Fig. 1). Among them, two patients had 3 FL, one 4 FL, and one more than 10 FL (Table 3). No association was established between MRI and PET for diffuse BMI detection ($p = 0.136$) in the SMM population, and PET detected more diffuse BMI than MRI (36% vs. 22%) (Fig. 3).

EMD was never detected in the whole population. Five/16 (31%) of the symptomatic MM patients had PMD detected each time by both PET and MRI imaging with equal numbers of lesions. PMD was never detected in SMM patients (Table 3).

Quantitative features

Quantitative features recorded by PET and MRI imaging are presented in Table 4. Median ADC_{mean}^{FL} was $768\mu m^2/s$ in the symptomatic MM patients and $727\mu m^2/s$ in SMM patients. Median ADC_{mean}^{BMI} was $467\mu m^2/s$ in both groups.

SUV_{max}^{BM} and ADC_{mean}^{BM} were weakly positively correlated ($r = 0.48$, $p = 0.00036$, Figure S1) whereas SUV_{max}^{FL} and ADC_{mean}^{FL} were not correlated (Figure S2). There was a trend to a negative correlation between SUV_{max}^{PMD} and ADC_{mean}^{PMD} ($r = -0.9$, $p = 0.083$, Figure S3), ADC_{mean}^{PMD} decreasing when SUV_{max}^{PMD} increased. In the total NDMM population, ROC analysis identified an optimal diagnostic MRI-based ADC_{mean}^{BM} cut-off value of $410\mu m^2/s$ for diffuse BMI detection with a

Table 2 Diagnostic performance of WB-2-[¹⁸F]FDG-PET/MRI imaging for FL and diffuse BMI detection in the total NDMM population and in individual SMM and symptomatic MM groups

Total NDMM population (n = 52)	FL	Diffuse BMI	FL and diffuse BMI	Diffuse BMI only	No abnormality
WB-2-[¹⁸ F]FDG-PET/MRI					18/52 (35%)
Positive	20/52 (38%)	26/52 (50%)	11/52 (21%)	15/52 (29%)	
Negative	32/52 (62%)	26/52 (50%)	41/52 (79%)	37/52 (71%)	
PET					24/52 (46%)
Positive	15/52 (29%)	23/52 (44%)	9/52 (17%)	12/52 (23%)	
MRI					25/52 (48%)
Positive	20/52 (38%)	18/52 (35%)	11/52 (21%)	6/52 (11%)	
SMM population (n = 36)	FL	Diffuse BMI	FL and diffuse BMI	Diffuse BMI only	No abnormality
WB-2-[¹⁸ F]FDG-PET/MRI					17/36 (47%)
Positive	8/36 (22%)	13/36 (36%)	4/36 (11%)	10/36 (28%)	
Negative	28/36 (78%)	23/36 (64%)	32/36 (89%)	26/36 (72%)	
PET					22/36 (61%)
Positive	4/36 (11%)	13/36 (36%)	2/36 (5%)	9/36 (25%)	
MRI					23/36 (64%)
Positive	8/36 (22%)	8/36 (22%)	3/36 (8%)	4/36 (11%)	
Symptomatic MM population (n = 16)	FL	Diffuse BMI	FL and diffuse BMI	Diffuse BMI only	No abnormality
WB-2-[¹⁸ F]FDG-PET/MRI					1/16 (6%)
Positive	12/16 (75%)	10/16 (62%)	10/16 (62%)	3/16 (19%)	
Negative	4/16 (25%)	6/16 (38%)	6/16 (38%)	13/16 (81%)	
PET					2/16 (12%)
Positive	11/16 (69%)	10/16 (62%)	7/16 (44%)	3/16 (19%)	
MRI					2/16 (12%)
Positive	12/16 (75%)	10/16 (62%)	8/16 (50%)	2/16 (12%)	

NDMM, newly diagnosed multiple myeloma; FL, focal lesion; BMI, bone marrow involvement; ND, newly diagnosed; WB, whole-body; 2-[¹⁸F]FDG, 2-¹⁸F-fluorodeoxyglucose; PET, positron emission tomography; MRI, magnetic resonance imaging

Table 3 Number of focal lesions and para-medullary disease detected in SMM and symptomatic MM patients by PET and MRI imaging

Imaging	Number of focal lesions							PMD		
	N=0	N=1	N=2	N=3	N=4	N=5 to 10	N>10	N=0	N=1	N=2
SMM (n = 36)										
PET (n)	32	1	1	0	0	1	1	0	0	0
MRI (n)	28	1	1	2	1	1	2	0	0	0
Symptomatic MM (n = 16)										
PET (n)	5	5	0	2	0	0	4	11	4	1
MRI (n)	4	3	0	1	0	1	7	11	3	2

SMM, smoldering multiple myeloma; MM, multiple myeloma; PMD, para-medullary disease

high specificity of 0.91 and a low sensitivity of 0.46 (area under curve: 0.71, Figure S4).

Discussion

We report here the first results concerning the added value of hybrid simultaneous WB-2-[¹⁸F]FDG-PET/MRI imaging in a prospective cohort of confirmed (according to IMWG)

NDMM patients. This new hybrid technique represents the most powerful and complementary imaging tool available in MM: within 1 h, imaging can provide clinicians with both serial diagnostic and prognostic data. Achieving a simultaneous WB-2-[¹⁸F]FDG-PET/MRI imaging protocol has a significant practical benefit for patients as they only have to attend the hospital/clinic once for a full imaging overview, only receive a low radiation dose, and only have to be imaged once.

Fig. 1 A 66-year-old man with a IgAκ multiple myeloma without criterion of therapy before the whole-body 2-[¹⁸F]FDG-PET/MRI imaging. Whole-body maximum intensity projection (MIP) PET image (a) shows no focal or diffuse bone marrow abnormality. Axial STIR images (b) show two focal bone lesions (size between 5 and 10 mm) of the left transverse process of T4 (red arrow) and the vertebral body of T9 (blue arrow) easily detectable in high 800 b-value axial diffusion weighted images and corresponding ADC mapping (c) which confirms the decrease of the apparent diffusion coefficient in these areas (mean value: 650 μm²/s). Fused corresponding axial PET/b800-DWI-MRI slices show the absence of increased FDG accumulation in these MRI detected focal bone lesions (d). Therapy was started according to IMWG criteria

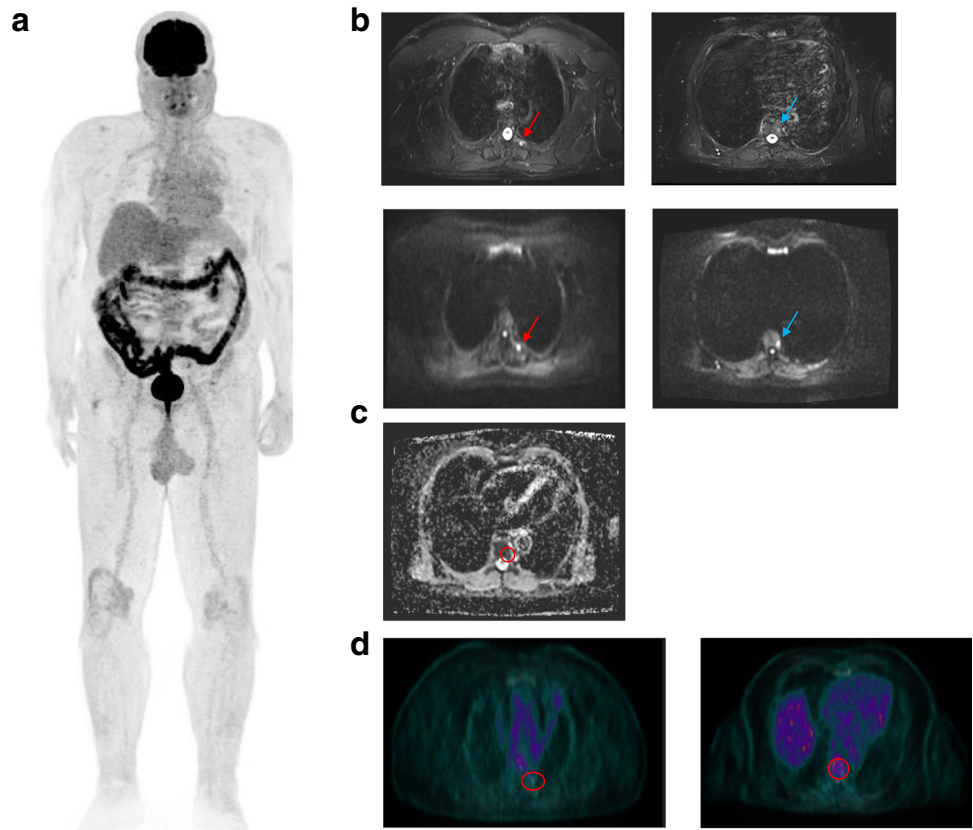


Fig. 2 A 61-year-old woman with a IgGκ multiple myeloma without criterion of therapy before the whole-body FDG-PET/MRI imaging. Involved/uninvolved serum free light chain ratio was borderline (98). Whole-body maximum intensity projection (MIP) PET image (a) shows a single hot spot in the pelvic bone. Axial PET and STIR images (b) show an active lesion of the right sacrum aileron in front of a 13-mm-diameter focal bone lesion. Fused corresponding axial PET/STIR-MRI slice (c) shows perfect matching between the PET and STIR abnormalities. ADC map (d) exhibits the decrease of the apparent diffusion coefficient in this hypercellular focal bone lesion (mean value: 791 μm²/s). Considering the size of this only focal bone lesion and the borderline serum free light chain ratio, therapy was triggered

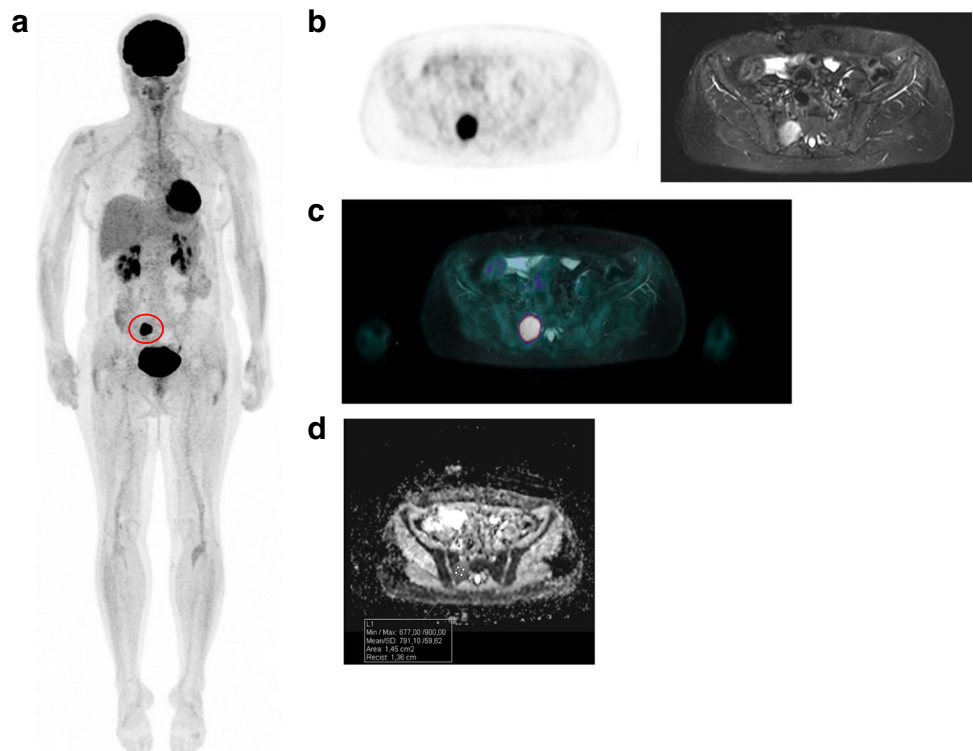


Fig. 3 A 44-year-old man with a IgGκ SMM. Whole-body maximum intensity projection (MIP) PET image (a) shows diffuse homogeneous bone marrow increase uptake (> hepatic background uptake). Sagittal PET/STIR/fused slices (b) confirm diffuse bone marrow uptake without corresponding medullary increase signal on STIR and without diffuse medullary decrease signal on T1-DIXON in-phase sagittal images (c). Axial b800-value diffusion weighted imaging (d) shows no bone marrow increase signal. As this patient had only diffuse bone marrow involvement without focal bone lesion detected in PET and MRI imaging, therapy was not started according to IMWG guidelines and he was only monitored

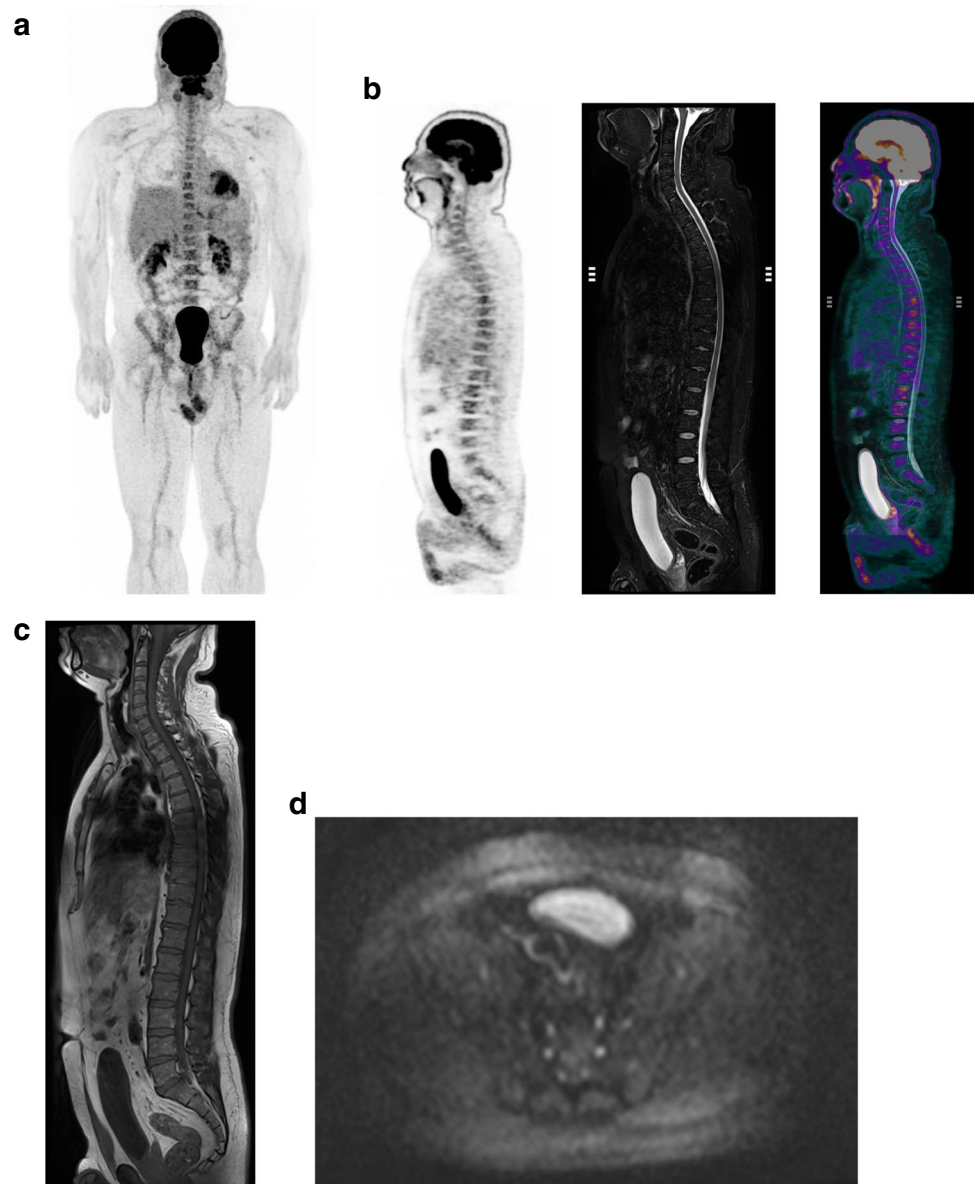


Table 4 Quantitative features recorded for PET and MRI imaging

Variable	Symptomatic MM <i>n</i> = 16	SMM <i>n</i> = 36
Median SUV_{max}^{FL}	7.49 (2.85 to 21.9)	10.26 (3.13 to 17.64)
Median SUV_{max}^{BMI}	4.68 (3.03 to 9.91)	4.02 (3.07 to 11.2)
Median SUV_{max}^{PMD}	7.89 (3.27 to 8.41)	N/A
Median ADC_{mean}^{FL}	768 (483 to 865)	727 (511 to 938)
Median ADC_{mean}^{BMI}	467 (220 to 711)	467 (347 to 540)
Median ADC_{mean}^{PMD}	816 (648 to 1467)	N/A

FL, focal lesion; *BMI*, bone marrow involvement; *PMD*, para-medullary disease; *MM*, multiple myeloma; SUV_{max} , maximum standardized uptake value; ADC_{mean} , mean value of apparent diffusion coefficient in $\mu m^2/s$

Focal bone lesion detection

In NDMM, detection of bone disease is one of the main goals of imaging. The presence of more than one $FL \geq 5$ mm by MRI imaging is a biomarker of malignancy, i.e., an MDE, triggering the start of therapy [1].

In this study, global WB-2- $[^{18}F]$ FDG-PET/MRI imaging detected at least one FL in 75% of patients with symptomatic MM which is consistent with classic epidemiology of this disease [16]. An association was established between MRI and PET for FL detection (75% vs. 69%, respectively, $p = 0.03$) in symptomatic MM patients, which is inconsistent with results previously published by Westerland et al. [17] in a NDMM cohort composed almost exclusively of symptomatic patients. In this study, PET and WB-MRI

(including DWI images) were obtained separately and WB-MRI detected significantly more patients with FL. It is possible that PET is more sensitive when performed simultaneously and precisely fused with MRI, thus facilitating an improved interpretation of abnormalities identified by PET. This assumption is supported by a recent preliminary study assessing WB-2- ^{18}F FDG-PET/MRI imaging in a retrospective heterogeneous population of patients with suspected or confirmed MM [18] (equal sensitivity of PET and MRI for FL detection).

In this study, global WB-2- ^{18}F FDG-PET/MRI imaging detected FL in 8/36 (22%) patients with SMM, resulting in a significant impact on clinical management in this population because all of these SMM patients subsequently received treatment: all had at least 2 FL ≥ 5 mm and 1 patient a single large FL with borderline serum free light chain ratio. No statistically significant association was reported between MRI and PET modalities for FL detection ($p=0.176$), and MRI detected more SMM patients with FL than PET (22% vs. 11%).

The decrease in lesion size, the increase in ADC's, or the disappearance of these supplemental MRI focal lesions were confirmed using the follow-up scans within the framework of therapy assessment to rule out the possibility of false-positive lesions. This is a novel finding and confirms the high diagnostic value of MRI including DWI for FL detection (especially small lesions) in early stages of this disease.

It is important to consider the complementarity of the MRI and PET data in order to obtain full benefit of hybrid WB-2- ^{18}F FDG-PET/MRI imaging. In addition to the diagnostic value of MRI and PET, the well documented important prognostic value of PET results should be also be mentioned. Indeed, recent large prospective and retrospective studies which assessed 2- ^{18}F FDG-PET/CT in NDMM showed several important results. Approximately 10% of patients with NDMM are 2- ^{18}F FDG-PET false-negative, this phenomenon being associated with low expression of hexokinase-2 [19], but these patients have a better prognosis than those with positive 2- ^{18}F FDG-PET [9]. Moreover, several PET-based biomarkers (number of FL > 3, high $\text{SUV}_{\text{max}}\text{FL}$ and/or high $\text{SUV}_{\text{max}}\text{BMI}$, presence of PMD or EMD) were repeatedly correlated with worse outcome [6–8, 10, 20–22] so are useful to report.

Follow-up of patients included in this cohort should allow to demonstrate that 2- ^{18}F FDG-PET results also have a prognostic value when PET is acquired simultaneously and fused with MRI instead of CT.

Diffuse bone marrow involvement

Global WB-2- ^{18}F FDG-PET/MRI imaging detected diffuse BMI in 62% of symptomatic MM patients which is less than previously reported (90%, [19]). When analyzed

alone, PET and MRI were equally effective (62% for both of them). In SMM patients, WB-2- ^{18}F FDG-PET/MRI imaging detected diffuse BMI in 36% of cases. No association was established between MRI and PET for diffuse BMI detection ($p=0.136$), and PET detected more diffuse BMI than MRI (36% vs. 22%) which is not in agreement with previously reported results [23]. This could be explained in part by the absence of clear standardization of MRI interpretation for diffuse BMI detection.

In this current study, we defined diffuse BMI by MRI imaging as a diffuse decreased signal on T1-in phase-DIXON weighted and diffuse increased signal throughout the marrow (relative to normal adjacent muscle) on high b -value DWI like in all other MRI studies and more generally as recommended by international guidelines [12]. However, patients with single diffuse mild increased signal throughout the marrow on high b -value DWI without decrease signal on T1-in phase-DIXON weighted images were not considered with diffuse BMI but more as unclear.

In our opinion, the prognostic value and the plasma cells' biological characterization of diffuse BMI at baseline in NDMM are more important than their diagnostic value. Indeed, patients with MM have, by definition, a significant bone marrow infiltration of clonal plasma cells, and diffuse bone marrow involvement is not a MDE [1]. Furthermore, we have recently shown that the intensity of the bone marrow's 2- ^{18}F FDG uptake was linearly correlated with survival of NDMM patients [10]; the higher the $\text{SUV}_{\text{max}}\text{BM}$ is, the shorter progression-free survival is. Others have shown that diffuse BMI identified by MRI imaging also seemed to be correlated with poor prognosis [24] even though they did not correlate this with 2- ^{18}F FDG-PET. Furthermore, Paschali et al. identified a correlation between the intensity of the bone marrow's 2- ^{18}F FDG uptake and clonal plasma cell morphology. $\text{SUV}_{\text{max}}\text{BM}$ was significantly lower for the group of good differentiation vs. intermediate/low differentiation of clonal plasma cells [25].

In our cohort, $\text{SUV}_{\text{max}}\text{BM}$ and $\text{ADC}_{\text{mean}}\text{BM}$ were weakly positively correlated, indicating that each feature brings different and complementary information. Finally, ROC curve analysis identified an optimal diagnostic MRI-based $\text{ADC}_{\text{mean}}\text{BM}$ cut-off value of $410 \mu\text{m}^2/\text{s}$ for diffuse BMI detection which matches perfectly with a previous study [18].

Conclusion

WB-2- ^{18}F FDG-PET/MRI could represent the next-generation imaging for MM. WB-2- ^{18}F FDG-PET/MRI imaging detected at least one FL in 75% of patients with

symptomatic MM, and PET and MRI were equally effective at identifying patients with FL. WB-2-[¹⁸F]FDG-PET/MRI imaging detected FL in 22% of patients with SMM (with a higher diagnostic performance for MRI), resulting in a significant impact on clinical management in this population. SUV_{max} and ADC_{mean} quantitative features were weakly or not correlated. PET could provide important prognostic data in addition to good diagnostic performance.

Supplementary information The online version contains supplementary material available at <https://doi.org/10.1007/s00330-023-09593-1>.

Funding This work has been supported in part by grants from the French National Agency for Research called “Investissements d’Avenir” IRON Labex n°ANR-11-LABX-0018-01 and INCa-DGOS-Inserm_12558 (SIRIC ILIAD).

Declarations

Guarantor The scientific guarantor of this publication is Françoise Kraeber-Bodere (FKB), head of Nantes University Hospital’s department of nuclear medicine.

Conflict of interest The authors declare no competing interests.

Statistics and biometry No complex statistical methods were necessary for this paper.

Informed consent Written informed consent was obtained from all subjects (patients) in this study.

Ethical approval Institutional review board approval was obtained.

Cohort overlap Some study subjects or cohorts have previously been reported in Benaniba L, Tessoulin B, Trudel S, et al The MYRACLE protocol study: a multicentric observational prospective cohort study of patients with multiple myeloma. *BMC Cancer*. 2019;19(1):855.

Methodology

- prospective
- diagnostic study
- performed at one institution

References

1. Rajkumar SV, Dimopoulos MA, Palumbo A et al (2014) International Myeloma Working Group updated criteria for the diagnosis of multiple myeloma. *Lancet Oncol* 15:e538–e548
2. Hillengass J, Usmani S, Rajkumar SV et al (2019) International Myeloma Working Group consensus recommendations on imaging in monoclonal plasma cell disorders. *Lancet Oncol* 20(6):e302–e312
3. Hillengass J, Fechtner K, Weber M-A et al (2010) Prognostic significance of focal lesions in whole-body magnetic resonance imaging in patients with asymptomatic multiple myeloma. *J Clin Oncol* 28(9):1606–10
4. Kastritis E, Mouloupoulos LA, Terpos E, Koutoulidis V, Dimopoulos MA (2014) The prognostic importance of the presence of more than one focal lesion in spine MRI of patients with asymptomatic (smoldering) multiple myeloma. *Leukemia* 28(12):2402–2403
5. Zamagni E, Nanni C, Gay F et al (2016) 18F-FDG PET/CT focal, but not osteolytic, lesions predict the progression of smoldering myeloma to active disease. *Leukemia* 30(2):417–422
6. Moreau P, Attal M, Caillot D et al (2017) Prospective evaluation of magnetic resonance imaging and [18F] fluorodeoxyglucose positron emission tomography-computed tomography at diagnosis and before maintenance therapy in symptomatic patients with multiple myeloma included in the IFM/DFCI 2009 trial: results of the IMAJEM study. *J Clin Oncol* 35(25):2911–2918
7. Zamagni E, Patriarca F, Nanni C et al (2011) Prognostic relevance of 18-F FDG PET/CT in newly diagnosed multiple myeloma patients treated with up-front autologous transplantation. *Blood* 118(23):5989–5995
8. Bartel TB, Haessler J, Brown TLY et al (2009) F18-fluorodeoxyglucose positron emission tomography in the context of other imaging techniques and prognostic factors in multiple myeloma. *Blood* 114(10):2068–2076
9. Abe Y, Ikeda S, Kitadate A et al (2019) Low hexokinase-2 expression-associated false-negative (18) F-FDG PET/CT as a potential prognostic predictor in patients with multiple myeloma. *Eur J Nucl Med Mol Imaging* 46(6):1345–1350
10. Jamet B, Morvan L, Nanni C et al (2021) Random survival forest to predict transplant-eligible newly diagnosed multiple myeloma outcome including FDG-PET radiomics: a combined analysis of two independent prospective European trials. *Eur J Nucl Med Mol Imaging* 48(4):1005–1015
11. Benaniba L, Tessoulin B, Trudel S et al (2019) The MYRACLE protocol study: a multicentric observational prospective cohort study of patients with multiple myeloma. *BMC Cancer* 19(1):855
12. Messiou C, Hillengass J, Delorme S et al (2019) Guidelines for acquisition, interpretation, and reporting of whole-body MRI in myeloma: myeloma response assessment and diagnosis system (MY-RADS). *Radiology* 291(1):5–13
13. Dutoit J, Vanderkerken M, Verstraete KL (2013) Value of whole body MRI and dynamic contrast enhanced MRI in the diagnosis, follow-up and evaluation of disease activity and extent in multiple myeloma. *Eur J Radiol* 82(9):1444–1452
14. Nanni C, Zamagni E, Versari A et al (2016) Image interpretation criteria for FDG PET/CT in multiple myeloma: a new proposal from an Italian expert panel. IMPeTUs (Italian Myeloma criteria for PET USe). *Eur J Nucl Med Mol Imaging* 43(3):414–421
15. Messiou C, Collins DJ, Morgan VA, Desouza NM (2011) Optimising diffusion weighted MRI for imaging metastatic and myeloma bone disease and assessing reproducibility. *Eur Radiol* 21(8):1713–1718
16. Kyle RA, Gertz MA, Witzig TE et al (2003) Review of 1027 patients with newly diagnosed multiple myeloma. *Mayo Clin Proc* 78:21–33
17. Westerland O, Amlani A, Kelly-Morland C et al (2021) Comparison of the diagnostic performance and impact on management of 18F-FDG PET/CT and whole-body MRI in multiple myeloma. *Eur J Nucl Med Mol Imaging* 48(8):2558–2565
18. Burns R, Mulé S, Blanc-Durand P et al (2021) Optimization of whole-body 2-[¹⁸F]FDG-PET/MRI imaging protocol for the initial staging of patients with myeloma. *Eur Radiol* 32(5):3085–3096
19. Rasche L, Angtuaco E, McDonald JE et al (2017) Low expression of hexokinase-2 is associated with false-negative FDG-positron emission tomography in multiple myeloma. *Blood* 130(1):304
20. Aljama MA, Sidiqi MH, Buadi FK et al (2018) Utility and prognostic value of 18F-FDG positron emission tomography-computed tomography scans in patients with newly diagnosed multiple myeloma. *Am J Hematol* 93(12):1518–1523
21. Jung S-H, Kwon SY, Min J-J et al (2019) 18F-FDG PET/CT is useful for determining survival outcomes of patients with

- multiple myeloma classified as stage II and III with the revised international staging system. *Eur J Nucl Med Mol Imaging* 46(1):107–115
22. Michaud-Robert AV, Zamagni E, Carlier T et al (2020) Glucose metabolism quantified by SUV_{max} on baseline FDG-PET/CT predicts survival in newly diagnosed multiple myeloma patients: combined harmonized analysis of two prospective phase III trials. *Cancers (Basel)* 12(9):2532
23. Cavo M, Terpos E, Nanni C et al (2017) International Myeloma Working Group. Review Role of ^{18}F -FDG PET/CT in the diagnosis and management of multiple myeloma and other plasma cell disorders: a consensus statement by the International Myeloma Working Group. *Lancet Oncol* 18:e206-2017
24. Mouloupoulos LA, Dimopoulos MA, Christoulas D et al (2010) Diffuse MRI marrow pattern correlates with increased angiogenesis, advanced disease features and poor prognosis in newly diagnosed myeloma treated with novel agents. *Leukemia* 24:1206–1212
25. Paschali A, Panagiotidis E, Triantafyllou T et al (2021) A proposed index of diffuse bone marrow [^{18}F]-FDG uptake and PET skeletal patterns correlate with myeloma prognostic markers, plasma cell morphology, and response to therapy. *Eur J Nucl Med Mol Imaging* 48(5):1487–1497

Publisher's note Springer Nature remains neutral with regard to jurisdictional claims in published maps and institutional affiliations.

Springer Nature or its licensor (e.g. a society or other partner) holds exclusive rights to this article under a publishing agreement with the author(s) or other rightsholder(s); author self-archiving of the accepted manuscript version of this article is solely governed by the terms of such publishing agreement and applicable law.